Phys. Status Solidi A **207**, No. 2, 417–422 (2010) / **DOI** 10.1002/pssa.200925109

physica status solidi a
www.pss-a.com
applications and materials science

Luminescent characteristics of praseodymium-doped zinc aluminate powders

C. D. Hernández-Pérez[1], M. García-Hipólito[1], M. A. Álvarez-Pérez[2], O. Álvarez-Fregoso*[,1], F. Ramos-Brito[3], and C. Falcony[4]

[1] Instituto de Investigaciones en Materiales, Universidad Nacional Autónoma de México, AP 70-360 Coyoacán, 04510 México, DF, Mexico
[2] Facultad de Odontología, Universidad Nacional Autónoma de México, AP 70-360 Coyoacán, 04510 México, DF, México
[3] Laboratorio de Materiales Optoelectrónicos, DIDe, Centro de Ciencias de Sinaloa, Av. De las Américas No. 2771 Nte. Col. Villa Universidad, Culiacán, Sinaloa, 80010 México, C.P., Mexico
[4] Centro de Investigaciones y Estudios Avanzados del IPN, Departamento de Física, PO Box 14-7400, 7000 México, DF, Mexico

Received 5 March 2009, revised 26 September 2009, accepted 30 September 2009
Published online 17 November 2009

PACS 61.05.cp, 68.37.Hk, 78.55.Hx, 78.60.Hk, 81.15.Rs

* Corresponding author: e-mail oaf@servidor.unam.mx, Phone: 0155 56224649, Fax: 0155 56161371

In this research, we report the cathodoluminescence (CL) and preliminary photoluminescence (PL) properties of praseodymium-doped zinc aluminate powders. $ZnAl_2O_4$:Pr powders were synthesized by a very simple chemical process. X-ray diffraction spectra indicated a cubic spinel crystalline structure with an average crystallite size of 15 nm. CL properties of the powders were studied as a function of the praseodymium concentration and electron-accelerating potential. In this case, all the cathodoluminescent emission spectra showed main peaks located at 494, 535, 611, 646, and 733 nm, which were associated to the electronic transitions $^3P_0 \rightarrow {}^3H_4$, $^3P_0 \rightarrow {}^3H_5$, $^3P_0 \rightarrow {}^3H_6$, $^3P_0 \rightarrow {}^3F_2$, and $^3P_0 \rightarrow {}^3F_4$ of the Pr^{3+} ions, respectively. A quenching of the CL, with increasing doping concentration, was observed. Also, an increment on cathodoluminescent emission intensity was observed as the accelerating voltage increased. The PL emission spectrum showed similar characteristics to those of the CL spectra. The chemical composition of the powders, as determined by energy dispersive spectroscopy, is also reported. In addition, the surface morphology characteristics of the powders are shown.

1 Introduction In recent years, the studies on luminescent materials have gained more and more attention. Some types of materials that are important for this phenomenon are spinel structures. These materials comprise a very large group of structurally related compounds [1–4], many of them are of considerable technological or geological importance [5]. Spinel structures exhibit a wide range of electronic and magnetic properties [4]. The normal spinel is a typical example of a material with the general formula $(X)[Y]_2O_4$, where X and Y are divalent and trivalent ions, respectively, and the () and [] refer to the 8 tetrahedrally coordinated A sites and 16 octahedrally coordinated B sites, respectively, within the cubic cell. This material shows a close-packed face centered cubic structure with *Fd3m* space group symmetry [3] with wide bandgaps >3.5 eV. In particular, $ZnAl_2O_4$ presents a bandgap of 3.8 eV [6], which makes it transparent for light possessing wavelengths >320 nm [7], these characteristics allow it to be used as a host lattice for applications in thin-film electroluminescent displays [8], mechanical–optical stress sensors, and stressing imaging device [9]. On the other hand, this material has good catalytic properties such as cracking, dehydration, and dehydrogenation [10–12]. The spinel zinc aluminates have been widely used as ceramic, electronic materials in the chemical and petrochemical industries [13, 14], and more recently as transparent conductors. A few years ago, there was marked interest in the development of rare-earth (RE)-doped oxide-based phosphors for field emission displays (FEDs) because of their excellent chemical stability under electron bombardment, their relative high emission intensity, and their color-rendering index properties. Some attention has been paid to the luminescence properties of

© 2010 WILEY-VCH Verlag GmbH & Co. KGaA, Weinheim

RE-ion-doped zinc aluminate and its possible application as a phosphor for FEDs. The electronic structures of the RE ions are characterized by their incompletely filled 4f shell. The 4f electrons lie inside the ion and are shielded by filled 5s and 5p electron orbitals [15, 16]. When these materials are excited by various means, intense sharp-line emissions are observed due to intra-4f-shell transitions of RE ion cores [17–22]. Recently, some attention has been paid to the luminescence properties of RE-doped zinc aluminate spinels, for example, this host lattice has been doped with Tb^{3+}, Tm^{3+}, Eu^{3+}, Dy^{3+}, Sm^{3+}, and Ce^{3+} ions [23–30]. The trivalent praseodymium ion, when embedded in this crystalline environment, exhibits rich line emission spectra originated by transitions within the states of the $4f^2$ ground configuration. Moreover, the parity-allowed electric-dipole-type $4f5d \rightarrow 4f^2$ transitions are known to result in intense emission bands with very fast decay times [31]. In general, there are several studies on the $5d^1 4f^{n-1}$–$4f^n$ transition of Pr^{3+} in crystals. The state $5d^1 4f^{n-1}$ configuration arises due to the coupling of $4f^{n-1}$ and $5d^1$ configurations that is allowed by parity and therefore the absorption and luminescence bands ascribed to these transitions are intensive, substantially broadened and in consequence, the Stokes shift of luminescence is extended to several thousand cm^{-1} [32].

In previous studies, we have obtained photoluminescence (PL) from Ce, Eu, and Tb ion-doped zinc aluminate coatings by using a spray-pyrolysis technique [26, 27, 33]. Our results showed that zinc aluminate is a good host material for the RE ions mentioned. In order to continue the research on RE-ion-doped zinc aluminate phosphors in a powder form, we resolve to implement, for the synthesis of samples, a simple chemical method that presents a great advantage over others preparation techniques due to powders are formed directly from the start mixture or solution, polycrystalline or amorphous powders can be obtained; it is also possible to control particle size, particle shape, chemical composition, stoichiometry, etc. Moreover, in many cases, these powders do not need high annealing temperature and milling processes. Lastly, it is convenient to mention that cathodoluminescence (CL) is an important technological phenomenon that is most widely used in modern cathode-ray tube (CRT) based instruments, and recently it has emerged as an important microcharacterization tool for the analysis of luminescent materials.

In this contribution, we reported the CL characteristics of $ZnAl_2O_4$:Pr^{3+} powders as a function of doping concentration and electron-accelerating voltage. In addition, preliminary PL results are reported. Also, chemical composition measurements and surface morphology micrographs of the synthesized powders are shown.

2 Experimental details A very simple chemical process was used for the synthesis of $ZnAl_2O_4$:Pr^{3+} powders. This simple process basically consists of three steps: (1) precursor material dissolution in a compatible solvent to form the initial mixture, (2) solvent evaporation and solute precipitation, and (3) powder annealing. The start materials were Zn $(NO_3)_2 \cdot 6H_2O$, Sigma–Aldrich (98%); $Al(NO_3)_3 \cdot 9H_2O$, Riedel-de Haën at 0.05 M blended in methanol. Doping with praseodymium was achieved by adding $Pr(NO_3)_3 \cdot 6H_2O$ Alfa Æsar (99.9%) in the range from 0 to 10 at.%. The initial mixture was heat treated at 250 °C for 30 min to evaporate the solvent. The obtained chemical agglomerates were grounded in an agate mortar to obtain fine powders. All powders were annealed at $T_a = 600$ °C, for 14 h in an air atmosphere.

The crystalline structure of these powders was analyzed by X-ray diffraction (XRD) using a Bruker-D8 plus Diffractometer with Cu Kα radiation at 1.5405 Å. Their chemical composition was measured using energy dispersive spectroscopy (EDS) with a Cambridge-Leica Scanning Electron Microscope (SEM) Stereoscan 440 equipped with a Beryllium window X-ray detector; and the surface morphology was obtained by means of the above-mentioned SEM.

CL measurements were performed in a stainless steel vacuum chamber with a cold cathode electron gun (Luminoscope, model ELM-2; MCA, Relion Co.). Samples (pellets of 1.5 cm in diameter and 0.2 cm in thickness) were placed inside the vacuum chamber and evacuated to 10^{-2} Torr. The emitted light from the sample was coupled into an optical fiber bundle leading to a spectrofluorometer SPEX Fluoro-Max-P. All CL spectra were obtained at room temperature. The accelerating voltage of the electron beam, used in the measurements reported, was in the range from 4 to 14 kV and the applied current was kept constant at 0.05 mA. The spot size of the electron beam on the sample surface was approximately 3 mm in diameter. Preliminary PL measurements were carried out with a 257 nm wavelength, using the above-mentioned spectrofluorometer.

3 Results and discussion The crystalline structure of the $ZnAl_2O_4$ powder, after the annealing process, is shown in Fig. 1. It is possible to see the marked presence of

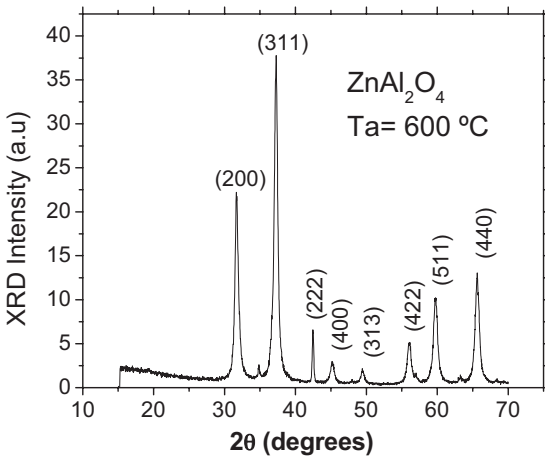

Figure 1 XRD pattern for praseodymium-doped zinc aluminate powder annealed at 600 °C for 14 h.

$ZnAl_2O_4$-gahnite face-centered cubic with spatial group *Fd*3*m* crystalline phase (ICCD Card File No. 065-3104). The presence of a crystalline ZnO trace is observed too, and it is evidenced from the low-intensity XRD peaks centered at 35° and 62°. The sharp profiles of the XRD peaks make evident the recrystallization and the consequent grain-growth process experienced by the material as a result of the annealing treatment. The calculated lattice parameter: $a = 8.0534 \pm 0.03$ Å, for cubic spinel phase in the samples annealed at 600 °C, is in good concordance with the reported value $a = 8.087$ Å. XRD patterns show peaks centered approximately at 32°, 37°, 42°, 45°, 49°, 56°, 60°, and 66° (2θ), that correspond to the diffracting planes: (2 2 0), (3 1 1), (2 2 2), (4 0 0), (3 1 3), (4 2 2), (5 1 1), and (4 4 0), respectively. A crystalline size average value of 15 nm was obtained by the Scherrer formula over (2 2 0) and (3 1 1) peaks.

Table 1 shows the EDS measurements for $ZnAl_2O_4:Pr^{3+}$ powders. This table summarizes the relative chemical content of oxygen, zinc, aluminum, and praseodymium present in the final powders as a function of the relative content of $Pr(NO_3)_3$ into its corresponding precursor mixture. The $Pr(NO_3)_3$ relative content values were 0, 0.5, 1, 3, 5, and 10 at.%. A reduction in the relative content of aluminum was observed with a slight increase in the relative contents of oxygen and praseodymium, when the $Pr(NO_3)_3$ value increases. Under these conditions, the relative content of zinc stays practically constant. According to these results, the praseodymium ions probably substitute the aluminum ions in the host lattice.

Figure 2 shows SEM micrographs of representative undoped and doped $ZnAl_2O_4$ powders. Specifically, Fig. 2a–c shows the morphology of $ZnAl_2O_4$:Pr (0.00 at.%), $ZnAl_2O_4$:Pr (0.35 at.%), and $ZnAl_2O_4$:Pr (2.15 at.%) powders, respectively. All SEM images show the irregular agglomeration adopted by the particles that form the powders. These agglomerates show a wide variety of forms and sizes, in general, all present sharp edges and sizes higher than 50 μm, which are mainly due to the grinding process.

Figure 3 shows the behavior of the CL measurements on $ZnAl_2O_4:Pr^{3+}$ powders as a function of doping concentration. The accelerating voltage of the electron beam was

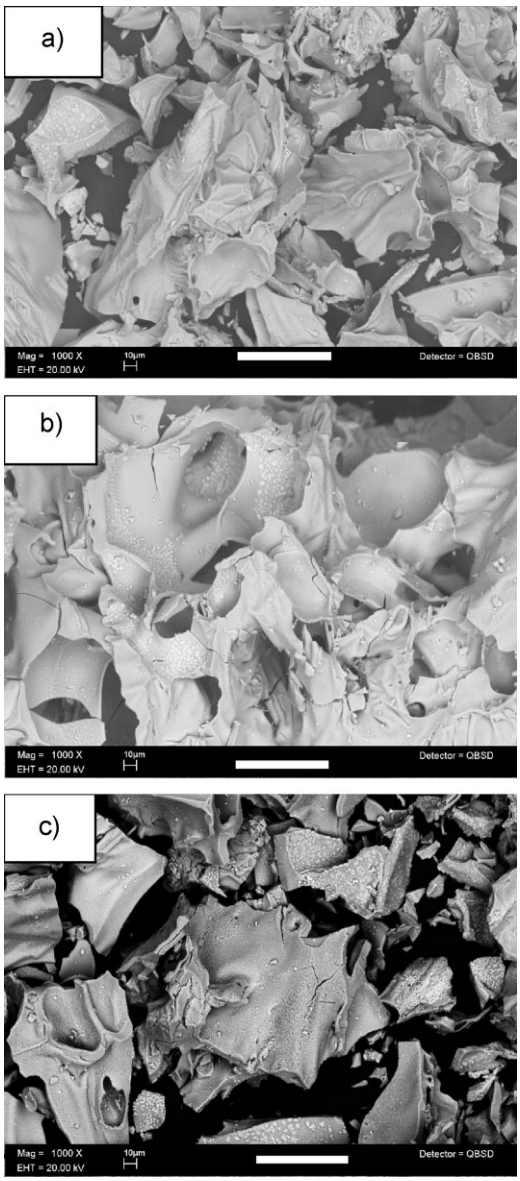

Figure 2 SEM micrographs for the surface morphologies of $ZnAl_2O_4$:Pr powders: (a) $ZnAl_2O_4$:Pr (0 at.%), (b) $ZnAl_2O_4$:Pr (0.35 at.%), and (c) $ZnAl_2O_4$:Pr (2.15 at.%). The white bars represent 50 μm.

Table 1 Atomic percent of the oxygen, zinc, aluminum, and praseodymium in the praseodymium-doped $ZnAl_2O_4$ powders as measured by EDS for different $Pr(NO_3)_3$ concentrations in the start mixture. In this case, the annealing temperature was 600 °C.

$Pr(NO_3)_3$ (at.%)	oxygen	zinc	aluminum	praseodymium
0	56.51	15.14	28.35	00.00
0.5	57.12	15.31	27.34	00.23
1	57.91	15.03	26.71	00.35
3	58.87	14.51	25.76	00.86
5	59.12	14.72	24.93	01.23
10	59.82	13.67	24.36	02.15

14 kV. The resulted emission spectra exhibit some dominant bands centered at 494, 535, 611, 646, and 733 nm, which are associated to the electronic transitions $^3P_0 \rightarrow {}^3H_4$, $^3P_0 \rightarrow {}^3H_5$, $^3P_0 \rightarrow {}^3H_6$, $^3P_0 \rightarrow {}^3F_2$, and $^3P_0 \rightarrow {}^3F_4$ of the Pr^{3+} ion, respectively. The strongest peak emission occurs at 646 nm. In fact, as the Pr^{3+} concentration increases the CL intensity also increases, but for doping concentration values higher than 0.35 at.% (as measured by EDS) a quenching effect is observed. The probable migration of the excitation by resonant energy transfer between the RE activators can be so efficient that it may carry the energy to a distant ion killer existing at some point of the luminescent material decreasing their emission intensity. Furthermore, aggregation of doping

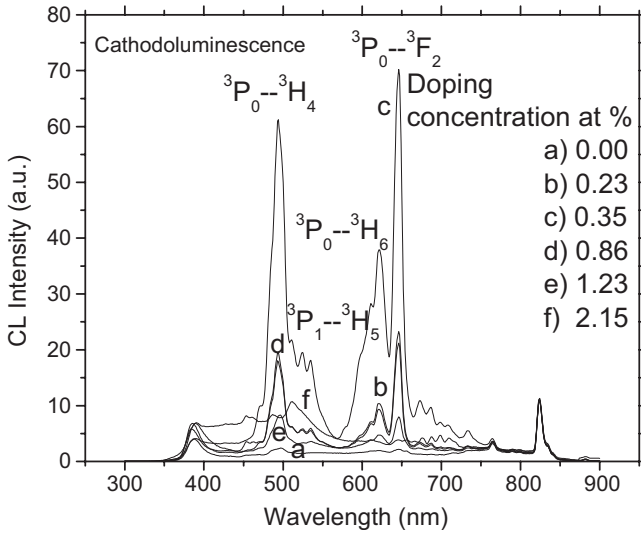

Figure 3 CL spectra for $ZnAl_2O_4$:Pr powders at different doping concentrations under 14 kV electron-accelerating voltage. $T_a = 600\,^{\circ}C$ annealed for 14 h.

activators at high concentrations may change some activators to quenchers and induce a related concentration quenching effect [34].

Figure 4 presents the CL measurements on the $ZnAl_2O_4$:Pr^{3+} (0.35 at.%) powder making variations in the electron-accelerating voltage. The measurements were obtained under steady-state excitation. The accelerating voltage was varied in the range from 4 to 14 kV. The shape of the emission spectra remains unaffected by the electron-accelerating voltage effect. All spectra show the same five main bands associated to trivalent praseodymium ions as was mentioned above. However, the overall emission intensity is larger for higher electron-accelerating voltage, showing no saturation effect in the voltage range studied.

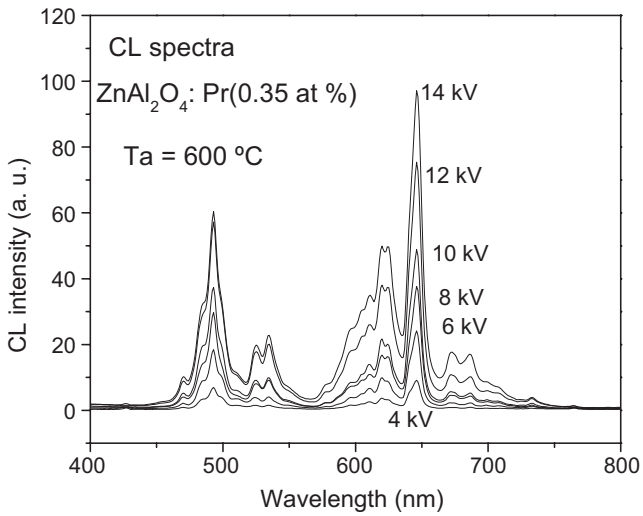

Figure 4 Behavior of CL emission intensity for $ZnAl_2O_4$:Pr (0.35 at.%) powders synthesized at $T_a = 600\,^{\circ}C$, for 14 h, as a function of the electron-accelerating voltage.

In CL spectroscopy, incident electrons interact with specimen atoms and are significantly scattered by them (rather than penetrating the sample in a linear fashion). Electrons that penetrate the sample can eject bound electrons, generating secondary electrons, or excite a valence electron to the conduction band, creating electron–hole pairs [35]. The quantity of secondary electrons and/or electron–hole pairs produced by an incident electron depends on its energy and the nature of the sample. The recombination of electron–hole pairs can produce photon emission. Therefore, as the electron-accelerating voltage increases, the penetrating electrons can produce more electron–hole pairs, due to the interaction with a larger volume of the luminescent material, to result in an increase of the CL intensity. Also, the production of secondary electrons is important to the CL-generation process, since they can generate electron–hole pairs along the entire electron zigzag path during its energy dissipation, which may be many micrometers in length [36]. The CL orange-reddish emissions could also be appreciated with the naked eye in normal room light, through the window of the CL chamber. The above-mentioned observation is a rough indication of the strength of the CL emissions.

Figure 5 shows the excitation spectrum for the $ZnAl_2O_4$:Pr^{3+} (0.35 at.%) powder at a monitored wavelength of 646 nm. There is a marked wide band centered at 257 nm and small peaks centered at 300, 322, 363, 382, and 395 nm. The broad band peaked at 257 nm may originate from the absorption of the matrix, namely, the band-to-band electronic transition of AlO_6 anion groups in the host lattice ($ZnAl_2O_4$), similar behavior has been observed in $ZnAl_2O_4$:Eu [37]. Probably, the small peaks centered at 300, 322, 363, 382, and 395 nm arise from the charge-transfer transition (CT) from coordination anions (O^{2-}) to the RE ions (Pr) or from the $4f^2 \rightarrow 4f5d$ transition of Pr^{3+} ion. Further experiments are now underway to give definitive assignments to these excitation bands.

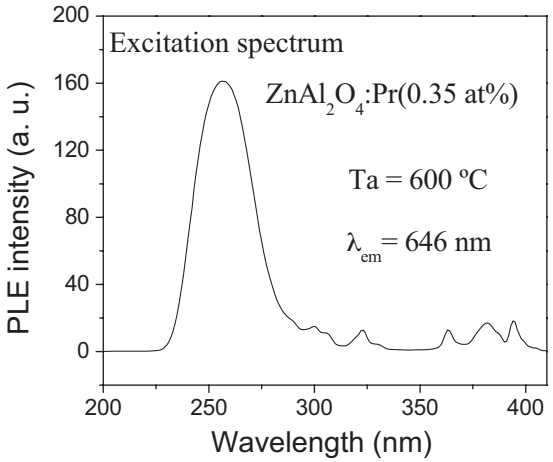

Figure 5 Excitation spectrum for $ZnAl_2O_4$:Pr (0.35 at.%) powders synthesized at 600 °C for 14 h ($\lambda_{em} = 646$ nm).

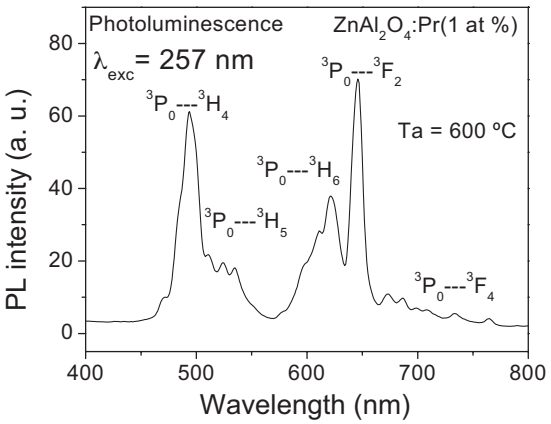

Figure 6 PL emission spectrum for $ZnAl_2O_4$:Pr (0.35 at.%) powders synthesized at 600 °C for 14 h ($\lambda_{exc} = 257$ nm).

The higher PL emission intensity under 257 nm excitation indicates more efficient energy transfer from the aluminate group toward the Pr^{3+} ions into the matrix. The CT transitions are present in RE ions, such as Eu^{3+} and Sm^{3+}, which are likely to be reduced. Furthermore, for trivalent RE ions having a clear tendency to become tetravalent, such as Pr^{3+} and Tb^{3+}, the 4f → 5d absorption band in the ultraviolet (UV) region is often observed [38]. Radiation with 257 nm wavelength was used to excite these powders.

Figure 6 shows the PL emission spectrum. The characteristics of this spectrum are very similar to those obtained for the CL measurements. An orange-reddish PL emission could easily be appreciated with the naked eye in normal room light, from $ZnAl_2O_4$:Pr samples when excited with a 4 W UV-mercury lamp (254 nm), which gives an idea, if not quantitatively at least qualitatively, of the strength of the PL emission.

4 Conclusions Intense visible reddish CL and PL emissions from praseodymium-doped $ZnAl_2O_4$ powders, synthesized by a simple chemical process, have been observed. XRD analysis on these powders showed that polycrystalline cubic phase of the $ZnAl_2O_4$ (gahnite) and small traces of crystalline ZnO are present in the powder. Using the Scherrer formula, an average crystallite size of 15 nm was estimated. The CL emission of the studied powders showed the characteristic peaks associated to intra-4f-shell transitions of Pr^{+3} ions. A CL emission intensity quenching was induced by increasing the doping concentration above its optimum value (0.35 at.%, as measured by EDS). Also, a continuous increase of the CL emission intensity was observed, as the electron-accelerating voltage increased. PL emission spectrum (excited by a wavelength of 257 nm) showed similar luminescent characteristics as compared to CL emission spectra. Therefore, this material could be a good candidate to be used in both applications involving photon- or electron-beam excitations.

Once again, it was confirmed that zinc aluminate is an efficient host lattice for RE ions as active centers to generate strong CL and PL luminescent emissions. Finally, it should be stressed that there are no reports in the literature, to the best of our knowledge, about the CL and PL characteristics of orange-reddish-emitting praseodymium-doped zinc aluminate powders.

Acknowledgements The authors thank L. Baños for XRD measurements and O. Novelo for SEM and EDS measurements. The technical support from M. Guerrero, Z. Rivera, and R. Reyes is also grateful. This research was supported by funds from DGAPA-PAPIIT-UNAM, project IN200808 to MAPP.

References

[1] E. J. Verwey and E. L. Heilmann, J. Chem. Phys. **15**, 174 (1947).
[2] E. W. Gorter, Philips Res. **9**, 295 (1954).
[3] R. J. Hill, J. R. Criag, and G. V. Gibbs, Phys. Chem. Miner. **4**, 317 (1979).
[4] R. E. Vandenberghe and E. deGrave, Mössbauer Spectroscopy Applied to Inorganic Chemistry, Vol. 3, edited by G. J. Long, and F. Grandjean (Plenum Press, New York, **1989**), p. 59.
[5] D. L. Anderson, Science **223**, 347 (1984).
[6] S. K. Sampath, D. G. Kanhere, and R. Pandey, J. Phys.: Condens. Matter **11**, 3635 (1999).
[7] S. Mathur, M. Veth, M. Hass, H. Shen, N. Lecerf, V. Huch, S. Hufner, R. Haberkorn, H. P. Beck, and M. Jilaib, J. Am. Ceram. Soc. **84**, 1921 (2001).
[8] G. Mueller, Electroluminescence II, Semiconductors and Semimetals, Vol. 65 (Academic Press, San Diego, 2000).
[9] H. Matsui, C.-N. Xu, and H. Tateyama, Appl. Phys. Lett. **78**, 1068 (2001).
[10] S. K. Sampath and J. F. Cordano, J. Am. Ceram. Soc. **81**, 649 (1988).
[11] W. S. Hong, L. C. De Jonghe, X. Yang, and M. N. Rahaman, J. Am. Ceram. Soc. **78**, 3217 (1995).
[12] A. K. Adak, A. Pathak, and P. Pramanik, J. Mater. Sci. Lett. **17**, 559 (1998).
[13] T. El-Nabarawy, A. A. Attia, and M. N. Alaya, Mater. Lett. **24**, 319 (1995).
[14] B. S. Girgis, A. M. Youssef, and M. N. Alaya, Surf. Technol. **10**, 105 (1980).
[15] J. F. Suyver, P. G. Kik, T. Kimura, A. Polman, G. Franzo, and S. Coffa, Nucl. Instrum. Methods Phys. Res. B **148**, 497 (1999).
[16] H. J. Lozykowski, W. M. Jadwisienczak, and I. Brown, J. Appl. Phys. **88**(1), 201 (2000).
[17] G. J. Kutcher, C. Burman, and R. Mohan, Int. J. Rat. Oncol., Biol. Phys. **20**, 127 (1991).
[18] F. M. Khan, The Physics of Radiation Therapy (Williams and Wilkins, London, 1984).
[19] C. K. Bomford, Text Book of Radiotherapy, 5th edition (Churchill Livingstone Medical Division of Longman Group, Elsevier Science Ltd., Edinburgh, United Kingdom, 1993).
[20] S. Koti, K. R. Reddy, V. G. Kakani, and D. Zhao, J. Exp. Bot. **56**(412), 725 (2005).
[21] G. A. Cardarelli, S. N. Rao, and D. Cail, Med. Phys. **18**(2), 282 (1991).
[22] P. A. Tanner, C. S. K. Mak, and M. D. Faucher, Chem. Phys. Lett. **343**, 309 (2001).
[23] E. Martínez-Sánchez, M. García-Hipólito, J. Guzmán, F. Ramos-Brito, J. Santoyo-Salazar, R. Martínez-Martínez, O.

Alvarez-Fregoso, M. Ramos-Cortés, J. Mendez-Delgado, and C. Falcony, Phys. Status Solidi A **202**, 102 (2005).
[24] W. Strek, P. Deren, A. Bednarkiewicz, M. Zawadzki, and J. Wrzyszcz, J. Alloys Compd. **300/301**, 456 (2000).
[25] M. Zawadzki, J. Wrzyszcz, W. Strek, and D. Hreniak, J. Alloys Compd. **323/324**, 279 (2001).
[26] M. García-Hipólito, A. Corona-Ocampo, O. Alvarez-Fregoso, E. Martínez, J. Guzmán-Mendoza, and C. Falcony, Phys. Status Solidi A **201**, 72 (2004).
[27] M. García-Hipólito, C. D. Hernández-Pérez, O. Alvarez-Fregoso, E. Martínez, J. Guzmán-Mendoza, and C. Falcony, Opt. Mater. **22**, 345 (2003).
[28] Z. Lou and J. Hao, Thin Solid Films **450**, 334 (2004).
[29] S. F. Wang, F. Gu, M. K. Mü, X. F. Cheng, W. G. Zou, G. J. Wang, S. M. Wang, and Y. Y. Zhou, J. Alloys Compd. **394**, 255 (2005).
[30] C. C. Yang, S. Y. Chen, and S. Y. Cheng, Powder Technol. **148**, 3 (2004).
[31] J. C. Gâcon, K. Horchani, A. Jouini, C. Dujardin, and I. Kamenskikh, Opt. Mater. **28**, 14 (2006).
[32] S. P. Chernov, L. I. Devyatkova, O. N. Ivanova, A. A. Kaminskii, V. V. Mikhailin, S. N. Rudnev, and T. V. Uvarova, Phys. Status Solidi A **88**, K 169 (1985).
[33] M. García-Hipólito, J. Guzmán-Mendoza, E. Martínez, O. Alvarez-Fregoso, and C. Falcony, Phys. Status Solidi A **201**(7), 1510 (2004).
[34] T. Hase, T. Kano, E. Nakasawa, and H. Yamamoto, Phosphor Materials for Cathode-Ray Tubes, in: Advances in Electronics and Electron Physics, Vol. 79, edited by P. W. Hawkes (Academic Press, New York, 1990), p. 271.
[35] L. Ozawa, Cathodoluminescence: Theory and Applications (Kodansha, Ltd., Tokyo, Japan and VCH Publishers, New York, USA, 1990), chap. 2.
[36] S. Myhajlenco, Luminescence of Solids, edited by D. R. Vij (Plenum Press, New York, 1998), chap. 4.
[37] B. Cheng, S. Qo, H. Zhou, and Z. Wang, Nanotechnology **17**, 2982 (2006).
[38] G. Blasse and B. C. Grabmaier, Luminescent Materials (Springer, Berlin, 1994), pp. 27–28.

